TU Delft

Delft University of Technology

A new design of a test platform for testing multiple partial discharge sources

Rodrigo Mor, A.; Castro Heredia, L.C.; Harmsen, D.A.; Muñoz, F.A.

DOI
10.1016/j.ijepes.2017.07.013

Publication date
2018

Document Version
Final published version

Published in
International Journal of Electrical Power & Energy Systems

Citation (APA)
Rodrigo Mor, A., Castro Heredia, L. C., Harmsen, D. A., & Muñoz, F. A. (2018). A new design of a test platform for testing multiple partial discharge sources. *International Journal of Electrical Power & Energy Systems*, *94*, 374-384. https://doi.org/10.1016/j.ijepes.2017.07.013

Important note
To cite this publication, please use the final published version (if applicable).
Please check the document version above.

Copyright
Other than for strictly personal use, it is not permitted to download, forward or distribute the text or part of it, without the consent of the author(s) and/or copyright holder(s), unless the work is under an open content license such as Creative Commons.

Takedown policy
Please contact us and provide details if you believe this document breaches copyrights.
We will remove access to the work immediately and investigate your claim.

This work is downloaded from Delft University of Technology.
For technical reasons the number of authors shown on this cover page is limited to a maximum of 10.

Electrical Power and Energy Systems 94 (2018) 374–384

Contents lists available at ScienceDirect

Electrical Power and Energy Systems

journal homepage: www.elsevier.com/locate/ijepes

A new design of a test platform for testing multiple partial discharge sources

A. Rodrigo Mor [a], L.C. Castro Heredia [a,*], D.A. Harmsen [a], F.A. Muñoz [b]

[a] Delft University of Technology, Electrical Sustainable Energy Department, Delft, The Netherlands
[b] Universidad del Valle, Escuela de Ingeniería Eléctrica y Electrónica, Cali, Colombia

ARTICLE INFO

Article history:
Received 25 January 2017
Received in revised form 13 June 2017
Accepted 17 July 2017
Available online 8 August 2017

Keywords:
Clustering techniques
Partial discharges
Phase resolved partial discharge pattern

ABSTRACT

Partial discharge (PD) measurements are an effective tool for insulation assessment of high-voltage (HV) equipment widely used in both HV laboratories and in field tests. This paper presents the design of a test platform for electrical detection of partial discharges that contribute to the understanding of the phenomena. The test set-up comprises a collection of electrodes for the production of artificial PD sources frequently found in HV equipment, such as positive corona, negative corona, surface discharges, internal discharges, floating component and free moving particle. The test set-up has been designed in such a way that the gaps and clearances can be adjusted to modify the discharge characteristics, e.g. the discharge inception voltage, amplitude, repetition rate, etc. Besides, the platform has a symmetrical and radial arrangement of the PD sources around the coupling capacitor of the PD measuring systems with contribute to reduce the effect of the measuring circuit on the measurements.

Relevant characteristics of the presented design is that the sensing of the PD signals is done by a high frequency current transformer (HFCT) with a wide bandwidth and the acquisition of the signals by a digital oscilloscope. A software tool was designed for the purpose of processing of the digitalized signals which proved to be an excellent workbench for studying the performance of clustering techniques.

© 2017 Elsevier Ltd. All rights reserved.

1. Introduction

Partial discharge (PD) measurement is a well-known diagnostic test for the dielectric insulation of HV equipment. Electrical detection of PD pulses is the most important and by far the most used method both in industrial and in laboratory tests. In addition to the conventional electrical methods as defined by standard IEC270 [1], currently the unconventional methods, understood as those with bandwidths lying on hundreds of MHz capable of resolve the waveform of the pulses, are becoming more and more predominant for testing cables, gas insulated systems and rotating machines [2–5]. One of challenges with the electrical detection is that a PD event itself cannot be measured directly but only the response of a measuring circuit after the PD event. In unconventional PD measuring systems, this response, i.e. the PD pulse waveform, is affected not only by the physics of the discharge but also by the interaction among the test object, the measuring circuit and the PD event. Consequently, PD parameters computed from the pulse waveform by different users and instruments might be incomparable.

As pointed out in [6], if properly measured, a PD pulse should be unipolar and non-oscillatory. However, If the test object has inductance as well as capacitance (e.g. a stator winding), then the PD pulse will create an oscillating response. Commonly, literature omits very deep details of the measuring circuit and readers are then prone to not to notice that even the connections and cables of measuring circuit affects the results. For instance, long lengths of cables in the circuit can add large ground inductances which produce an oscillatory response that affects the sensitivity [7] and the charge estimation [8] of the pulses.

In this paper, we present a design for an unconventional partial discharge test platform that contributes to minimize the aforementioned effects of the measuring circuit. This platform comprises several electrodes and a software tool to study different artificial PD sources representative of the most relevant insulation defects. It will be highlighted that the characteristics of the set-up contribute to control the circuit parameters, thus contributing to the repeatability and consistency of the measurements. Dimensions and details of the easy-to-build electrodes, a collection of phase-resolved PD patters (PRPD) as well as an introduction to the performance of clustering techniques to separate and recognize PD sources are provided to the user as a reference guide, that joins others efforts for a better learning of the PD phenomena [9,10].

* Corresponding author.
E-mail address: l.c.castroheredia@tudelft.nl (L.C. Castro Heredia).

http://dx.doi.org/10.1016/j.ijepes.2017.07.013
0142-0615/© 2017 Elsevier Ltd. All rights reserved.

2. Set-up description

A detailed scheme of the PD test platform is depicted in Fig. 1. The set-up comprises a high-voltage transformer, a blocking inductor, an arrangement of electrodes for different types of PD sources, a high frequency current transformer HFCT-type PD sensor, a high-voltage divider, a synchronization unit and an oscilloscope Tektronix DPO7354C.

2.1. High-voltage transformer supply

This set-up has been designed in such a way that the discharge inception voltage (DIV) is below 10 kV for any of the PD sources. In this way, a HV supply with proper ratings can be found in most cases. Due to the small currents, medium voltage instrument transformers can be used to energize the set-up. The high-voltage transformer is supplied from a regulating autotransformer via a safety box that includes a fence interlock, voltage and current trips. This transformer is located within a faraday cage (see square area D in Fig. 1a).

A blocking inductor is placed between the high-voltage transformer and the electrode arrangement to block possible discharges from the transformer and to increase the sensitivity of the set-up. The blocking inductor is a ten turns coil with a TDK N30 magnetic core.

2.2. Artificial PD sources

Several electrodes were built to create artificial PD sources such as positive corona, negative corona, surface discharges, internal

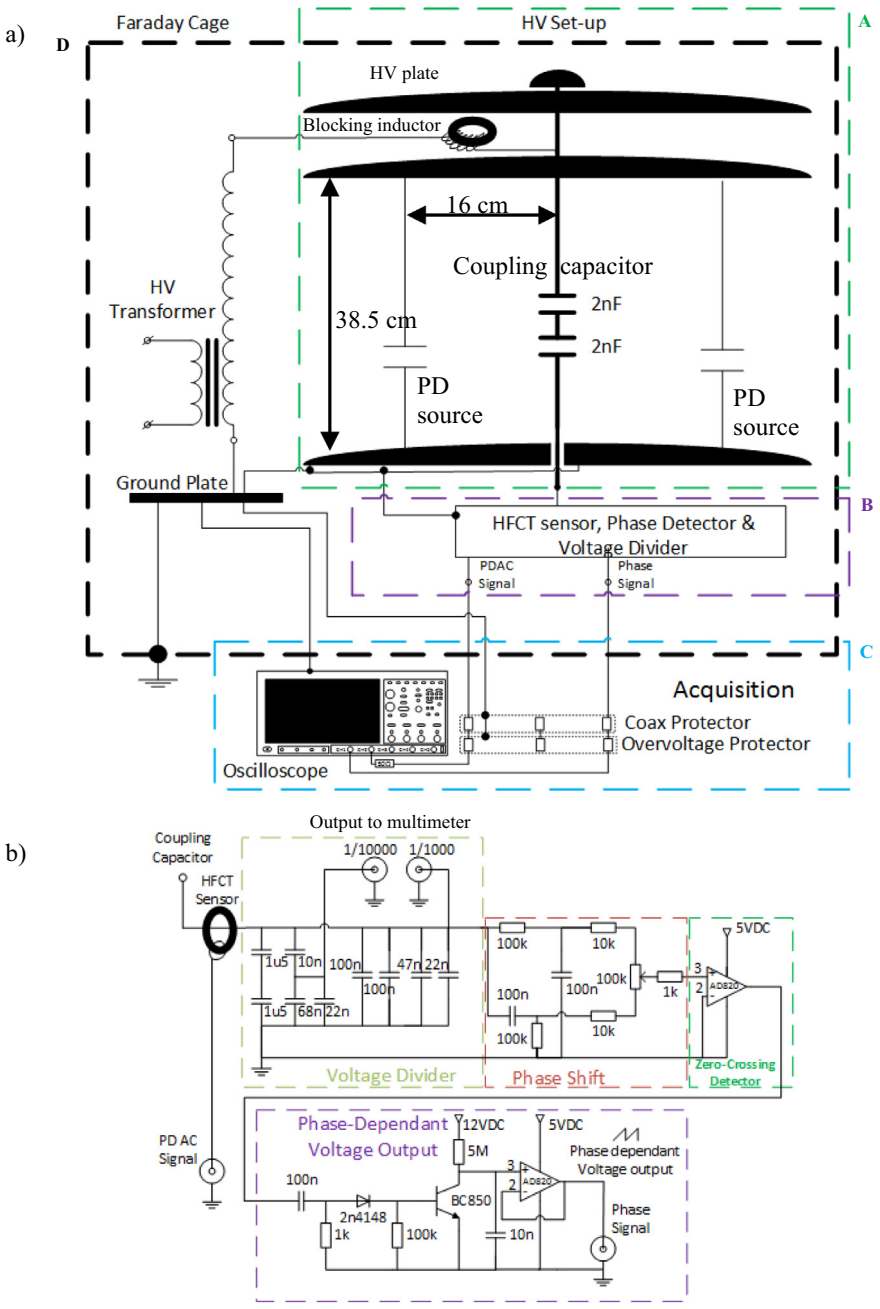

Fig. 1. (a) Scheme of the partial discharge test platform, (b) Circuitry of the synchronization unit, PD signals and voltage dividers arranged within the square area B. The square area A is the test set-up itself formed by the ground and high-voltage plates, the blocking inductor, the coupling capacitor and the PD sources.

discharges, floating electrode and free moving particle and they are located between the ground and high-voltage plates as illustrated within the square area A in Fig. 1a. The electrodes were designed using some of the ideas from [11–13]. Each source can be mounted and dismounted permitting to test single or multiple sources.

Each PD source shares the series of the two 2 nF capacitors as coupling capacitor in the center, as shown in Fig. 2. The two upper plates are connected to the high-voltage lead of the transformer and the bottom plate is the ground electrode, so anything connected to it will be earthed. Besides, the plates were given rounded profiles to avoid high electric field concentration. The height between the plates is 385 mm but it can be adjusted if needed by the nuts of the three nylon bolts serving as mechanical supports. The overall dimension of the set-up is 500 mm radius and 700 mm height. The scheme and picture of each PD source, including dimensions are shown in Figs. 3–5.

As can be noted, the electrodes (PD sources) are placed symmetrically and radially to the coupling capacitor. The radius is 16 cm. This arrangement provides physical and electrical symmetry of the circuit and the same current loop size for all the PD sources; this directly implies smaller current loops and therefore smaller inductances and higher cut-off frequencies. This arrangement also reduces the laboratory space dedicated to the set-up.

A particular characteristic of the set-up is that the dielectric clearances or gaps marked as *d* and *h* for each PD source can be adjusted as needed. For example, the needle length in the electrode of Fig. 3 can be adjusted to change the parameters of the discharge, including the discharge inception voltage. In the electrode of Fig. 4, the weight of the free moving particle affects the occurrence of discharges. For a given weight of the particle, the gap should be adjusted: if too short, the electric field can be so high that the particle will jump out of the electrode, if too long, the particle might not move at all.

It is noteworthy that in this paper positive or negative corona only refers to the electrode to which the needle is connected to, and not the polarity of the recorded pulses, e.g. for positive corona the needle is connected to the high-voltage electrode [14].

2.3. PD sensor

The test platform incorporates a high frequency current transformer (HFCT) for sensing the current of the PD pulses that is located within the connection box shown in square area B in Figs. 1a and 2. This HFCT consists of five turns wound onto a TDK N30 ferrite-core and terminated into 50 Ω resistor at the oscilloscope. Each turn was made of a flat copper strip 3 mm wide, taking care of having the turns evenly distributed along the core. Stray capacitances are reduced by using this configuration. The lower cut-off frequency at which the bandpass value of 9.416 mV/mA has fallen by 3 dB is 34.4 kHz, as highlighted in Fig. 6. As can be noted, the measurement of the upper cut-off frequency was hindered as the frequency reaches values over a few tens of MHz. At such high frequencies, the effect of resonances, stray capacitances and inductances in the straightforward measuring scheme implemented have a strong effect.

Alternatively, a calibration pulse was compared as recorded by the oscilloscope with a 500 MHz bandwidth and by the PD set-up. In the first case, a 1000 pC pulse was injected directly to the oscilloscope 50 Ω input and in the second case the pulse was injected between the ground and high-voltage plates of the PD set-up. From the comparison of the frequency spectra in Fig. 7, the upper cut-off frequency of the PD set-up was estimated at 60 MHz.

Although the fast calibration pulse is unipolar (as recorded by the oscilloscope), the interaction with the PD set-up produces an oscillation. Nevertheless, the bandwidth of the PD set-up is suitable for charge estimation methods and clustering techniques

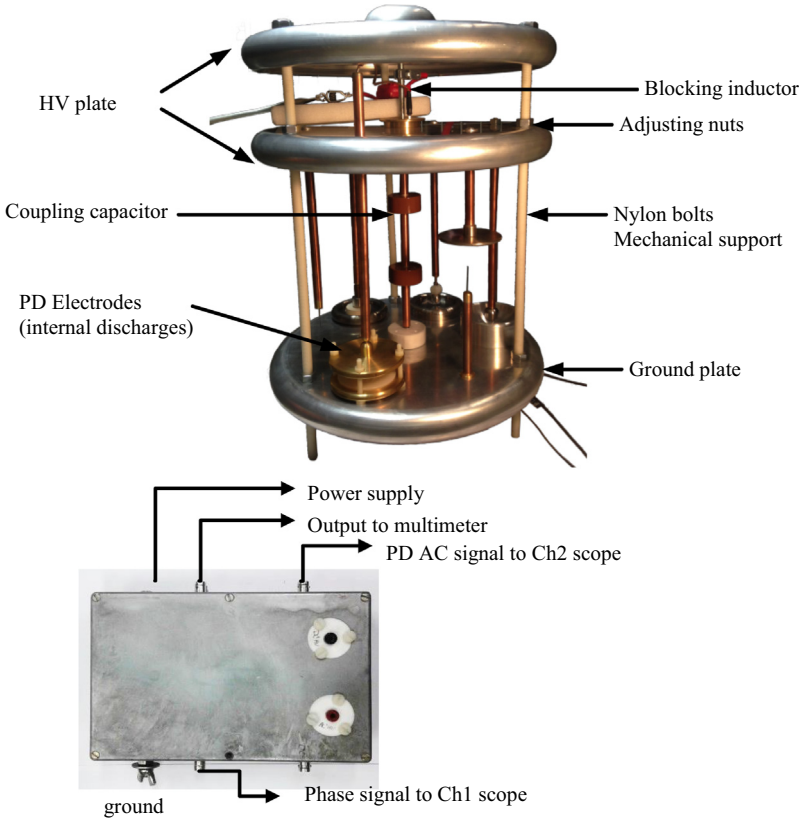

Fig. 2. The HV set-up with six artificial PD sources and the connection box containing all the circuitry illustrated in Fig. 1b.

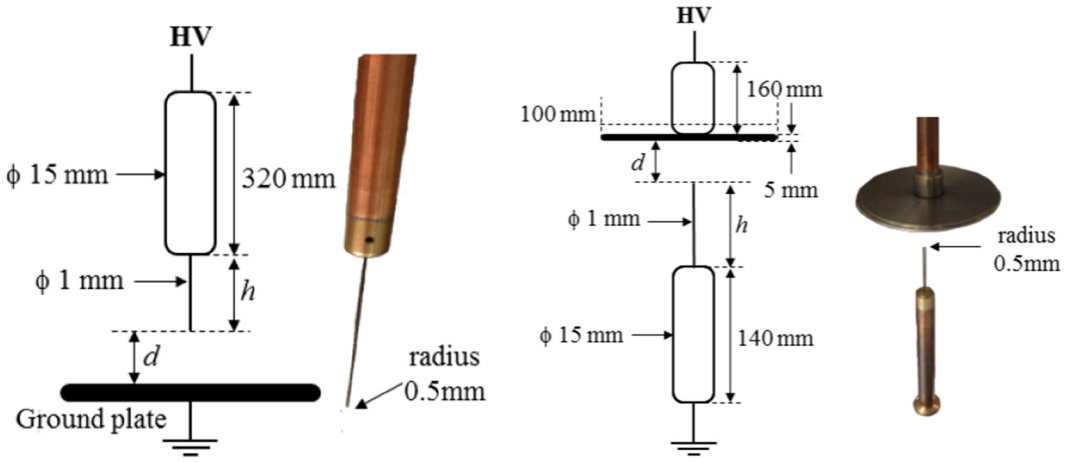

Fig. 3. (Left) Electrode for generating positive corona type PD pulses. The rod-needle is connected to the HV electrode. Reference dimensions: h = 20 mm, d = 45 mm. (Right) Electrode for generating negative corona type PD pulses. The rod-needle is connected to the ground electrode and the circular plate is connected to the HV plate. Reference dimensions: h = 45 mm, d = 40 mm. The length of the needle in both cases can be adjusted to change parameters of the discharge including the discharge inception voltage.

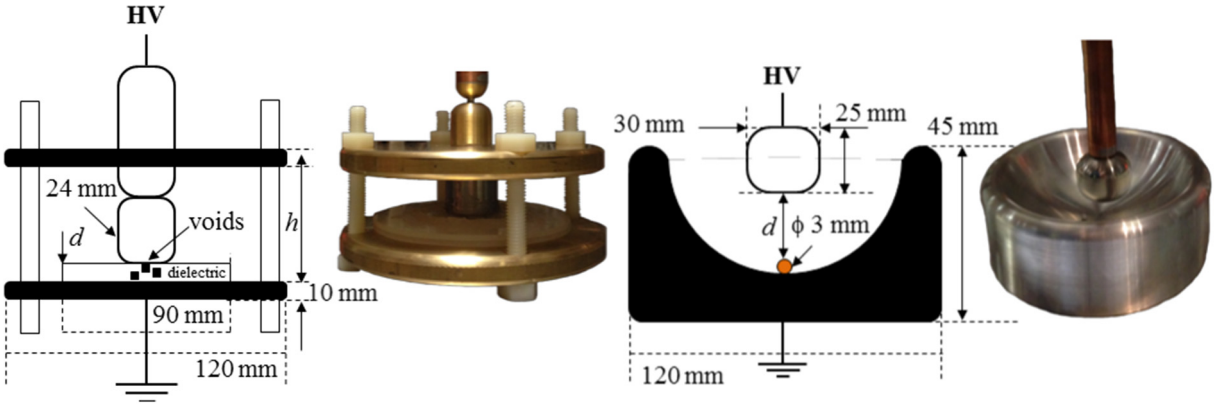

Fig. 4. (Left) Electrode for generating internal type PD pulses. The HV electrode pressures a dielectric sample (having voids) against the ground electrode. The height of electrode can be adjusted so dielectric samples of different thickness can be tested. Reference dimensions: d = 3 mm. (Right) Electrode for generating moving-particle type PD pulses. The moving-particle is a conductive ball. Reference dimensions: d = 13 mm, particle weight = 0.01 g.

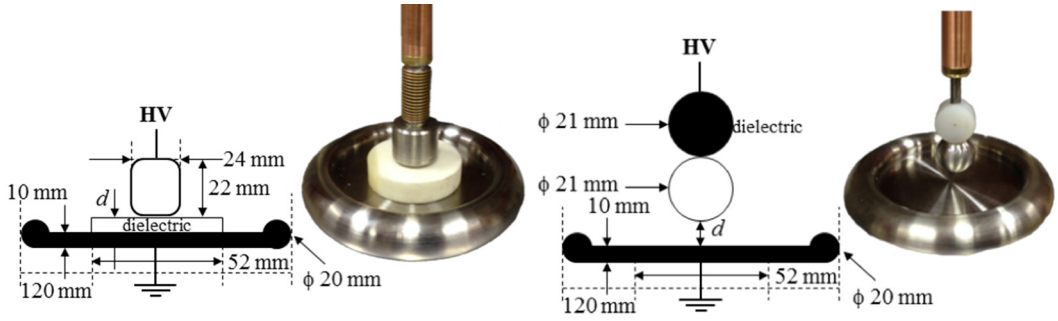

Fig. 5. (Left) Electrode for generating surface type PD pulses. Different HV electrodes having different edge radius can be used to change parameters of the surface discharge. There is a spring above the high-voltage electrode to assist the electric contact between the electrode and the dielectric sample. Reference dimensions: d = 12 mm. (Right) Electrode for generating floating-electrode type PD pulses. The HV rod and the floating metallic electrode are not electrically connected. Reference dimensions: d = 5 mm.

based on frequency spectrum analysis or time-domain calculations [15,16].

The polarity of the pulse at the output of the sensor depends on the direction of the current pulse flowing through the sensor core. Particularly, the current direction was chosen in such a way that for the positive corona type PD pulses, the recorded pulses will have negative polarity in the negative half cycle for consistency with the results reported in literature [14,17].

The performance of the PD set-up was tested by mean of the computation of errors in the charge estimation. To do so, calibrator pulses of different charge magnitude ranging from 10 pC to 5000 pC (500 pulses of each magnitude) were injected between the high-voltage and ground plates by using a Tettex Instruments calibrator. When injecting the calibration pulse, the capacitance of any of the PD sources is in the range of tens of picofarads therefore most of the current will flow through the 1 nF coupling

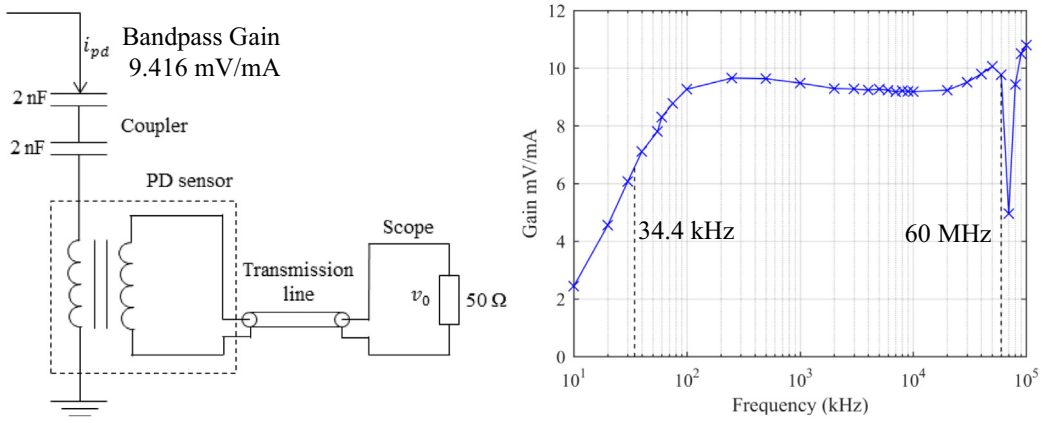

Fig. 6. Detection circuit made out of the HFCT sensor terminated at 50 Ω oscilloscope input. Frequency response of the PD sensor.

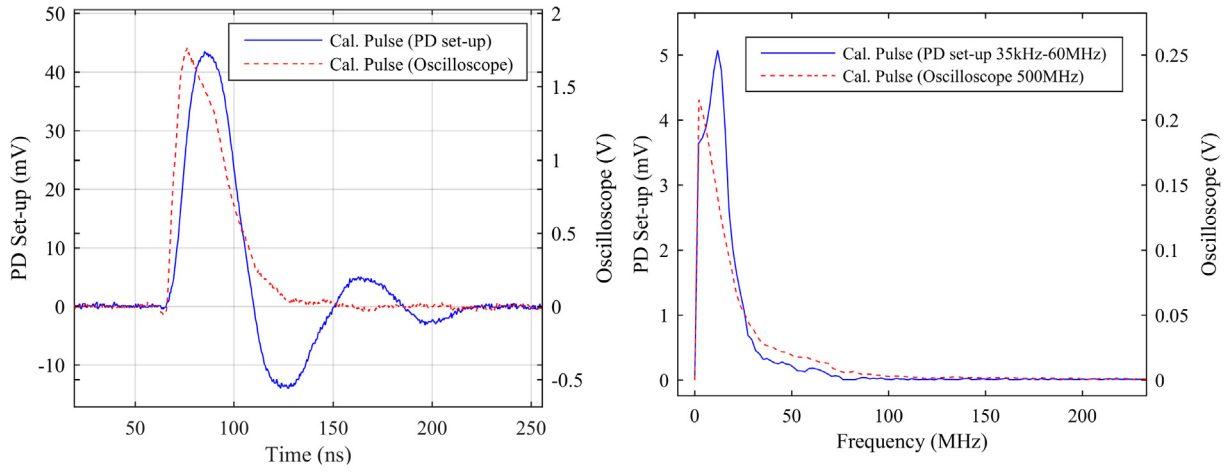

Fig. 7. Calibration pulse of 1000 pC and its frequency spectrum as measured by the PD set-up and by the digital oscilloscope.

capacitor to the sensor. Thus, the effect of having any of the PD sources connected during calibration is negligible.

The true charge of the calibrator pulses was calculated by injecting directly the pulses into the oscilloscope 50 Ω input and the solving the time integral of the current pulse [1,16]. The charge as estimated by the PD set-up was achieved following the IEC270 method. Nevertheless, other charge estimation algorithms can be used as the ones found in [8].

All the results are summarized in Table 1. As can be seen, the maximum error achieved by the PD set-up was around 9%.

2.4. High-voltage divider

A capacitive voltage divider is incorporated to measure the applied voltage, see Fig. 1b. The primary of the divider is the series of two 2 nF capacitors. These capacitors are TDK ceramic capacitors rated for 40 kV (DC) and tested PD free up to 15 kV (AC). The secondary of the divider, located within the connection box shown in Fig. 2 is formed by several series and parallel capacitors that offer attenuation ratios of 1/1000 and 1/10,000. The output of the divider can be directly connected to a high impedance voltmeter for easy reading of the applied voltage.

Table 1
Relative error achieved by the PD set-up.

Nominal charge [pC]	True charge [pC]	Estimated charge [pC]	Error [%]
10	9.7	8.9	−8.24
50	50.0	45.47	−9.06
100	99.5	104.15	4.67
500	495.4	526.44	6.26
1000	999.3	1006.65	0.73
5000	5076.5	5020.31	−1.10

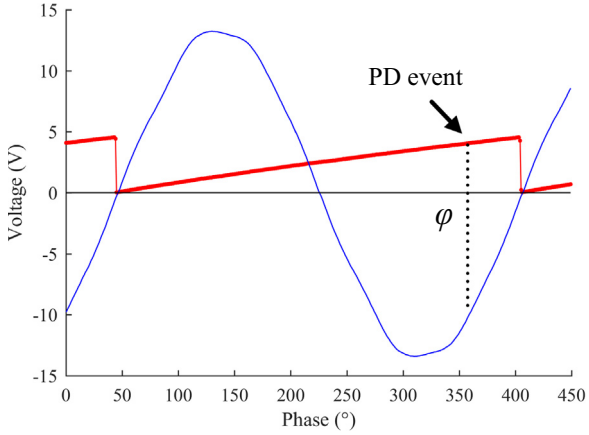

Fig. 8. Synchronization signal to acquire the phase of the PD pulses.

2.5. Synchronization unit

The PD pulse phase is acquired from the circuit shown in Fig. 1b that generates a sawtooth in phase with the AC applied voltage. Since

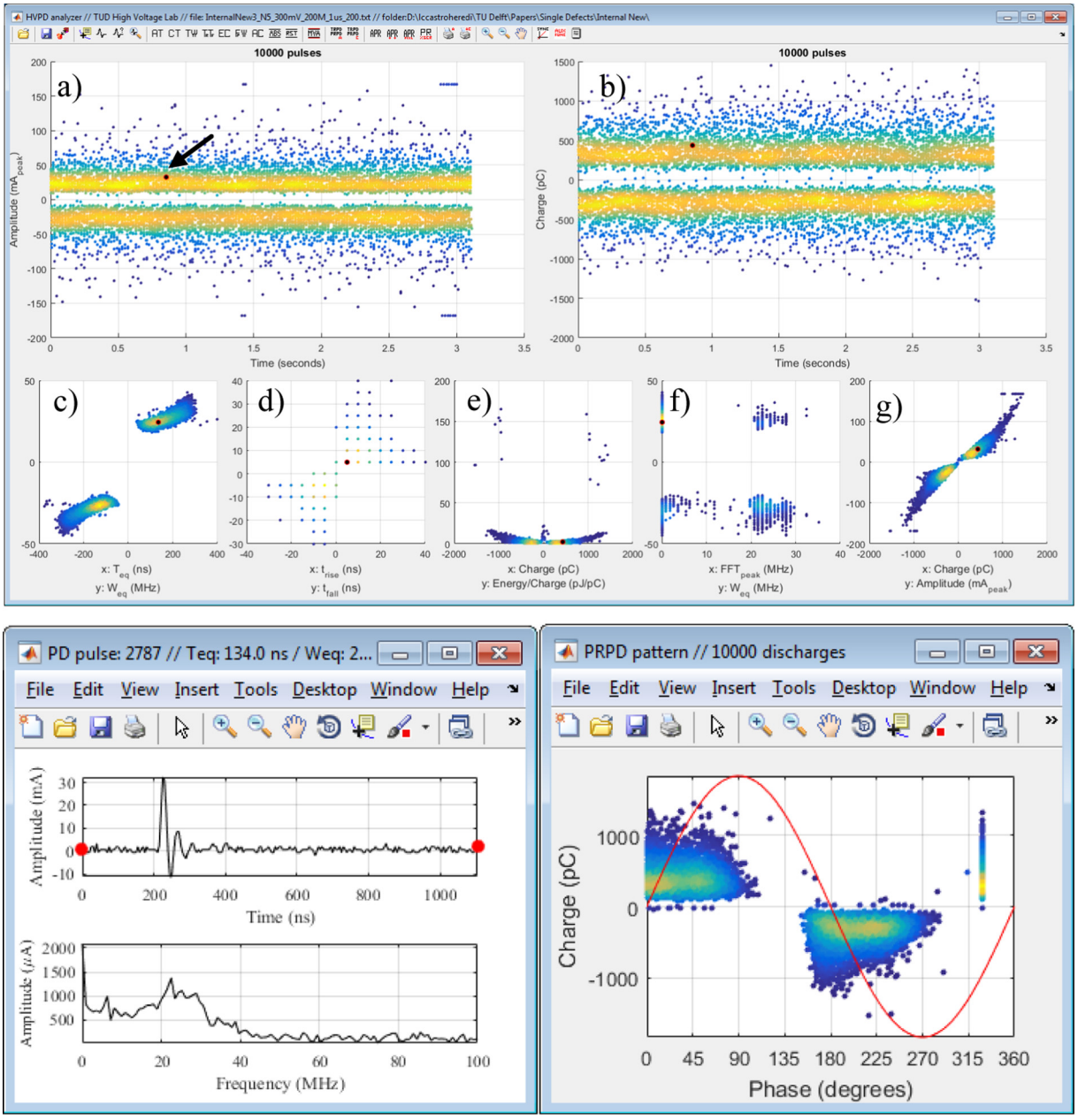

Fig. 9. GUI-based software tool (top). Pulse waveform and frequency spectrum of a single pulse chosen by the user (bottom-left) and the PRPD pattern (bottom-right).

the signal is triggered by a positive zero crossing point of the applied voltage, then the period of the sawtooth signal is the same as the period of the applied voltage. The slope of the ramp is steady through all of the period with an amplitude $\Delta V = 4.54$ V. When a PD event occurs, the oscilloscope records the PD signal and the values of the sawtooth signal at that instant. As depicted in Fig. 8, the phase of a PD pulse is proportional to the ramp voltage magnitude at which the PD pulse occurred. The trigger of the ramp by the zero crossing point of applied voltage enables to conduct tests with different frequencies of the test voltage. The circuit also includes a phase shift unit that compensates the phase delay of the voltage divider and the electronics, and it is tuned manually to minimum error.

2.6. Oscilloscope

A high performance oscilloscope Tektronix DPO7354C with 8 bits of vertical resolution. For the measurements here reported, a sampling frequency of 2.5 GS/s was used. After an acquisition, the time stamp data is saved to a txt file, and the PD pulses and the synchronization signal to a wfm file. A GUI-based software tool was developed to read the oscilloscope files and process the data off-line. This includes the computation of several clustering techniques and PRPD patters.

2.7. Background noise

As can be seen from Fig. 1a, the main set-up is located in a Faraday cage to reduce the background noise and external interferences. Before the utilization of the set-up, all the PD sources are disconnected and then the set-up is energized to check the background noise and external interferences displayed by the oscilloscope. For the particular case of the HV Laboratory of TU Delft, setting the window trigger level of the oscilloscope to above ±2.5 mV prevented the acquisition from being triggered by noise

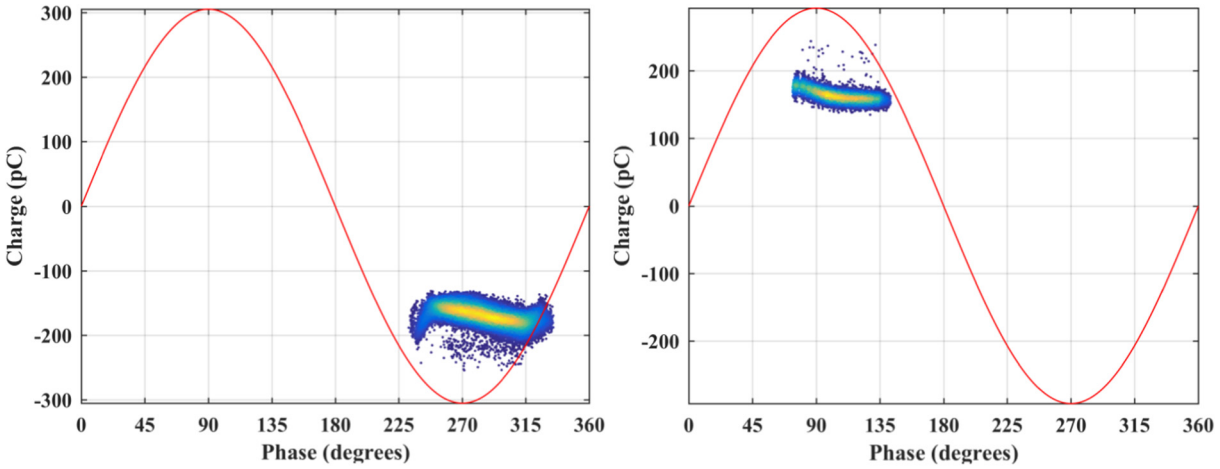

Fig. 10. (Left) Positive corona. (Right) Negative corona PRPD pattern.

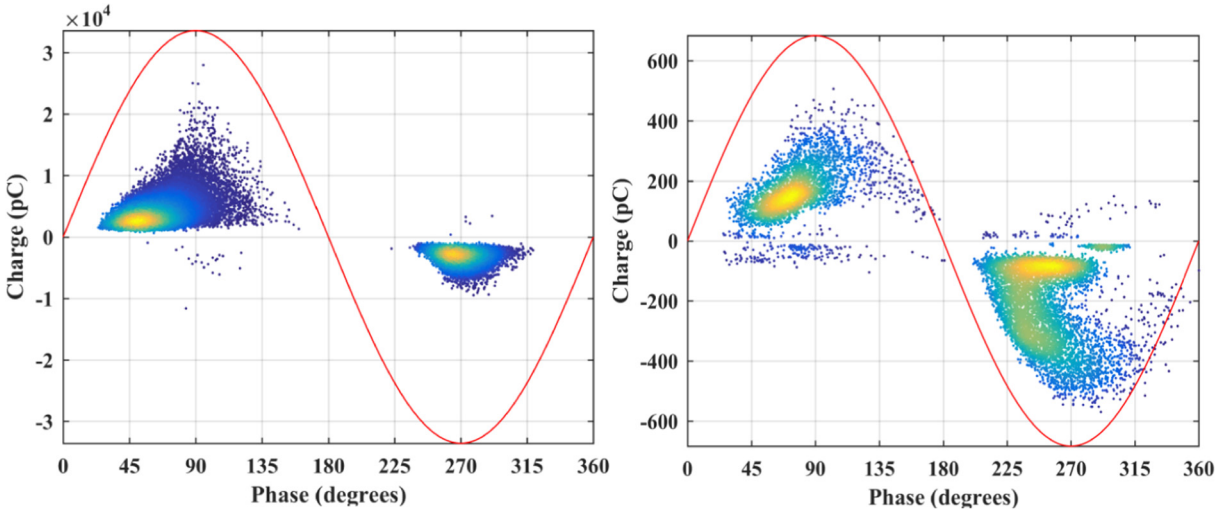

Fig. 11. (Left) Surface discharge. (Right) Internal discharge PRPD pattern.

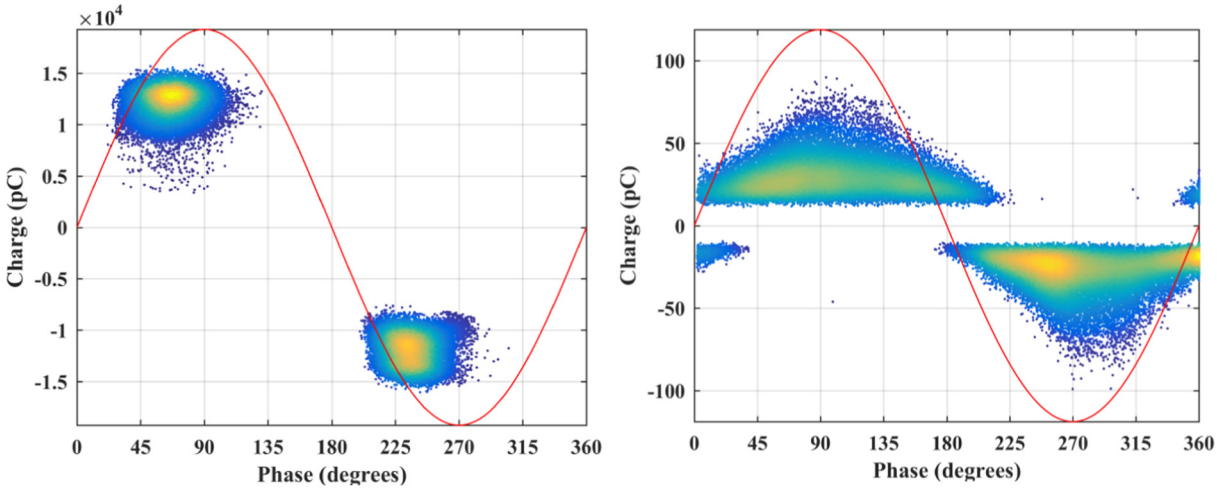

Fig. 12. (Left) Floating electrode. (Right) Floating particle PRPD pattern.

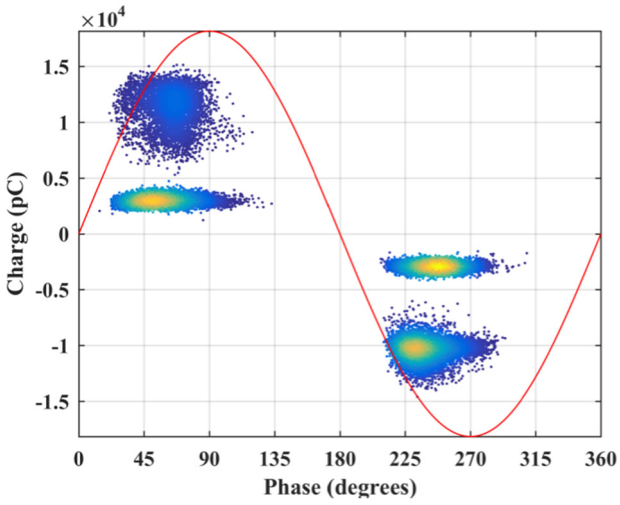

Fig. 13. PRPD pattern of surface and floating electrode combination.

signals but by the PD pulse signals. The sensitivity of the test platform is around 1 pC. Besides, the set-up was proven to be PD free up to the maximum test voltage of 10 kV.

3. Data acquisition and processing

The data acquisition unit used in this PD test platform is a Tektronix DPO7354C Digital Phosphor Oscilloscope. This oscilloscope was preferred due to its 'Fast Frame Acquisition Mode' which allows to capture all the trigger events as single records (a record is a frame) in a larger record. Therefore, each PD pulse can then be saved and processed individually. The memory management of the oscilloscope defines equal length for each record, e.g. depending on the sampling frequency and the acquisition time. This also means that whatever signal happens in between records is not acquired. Another important feature is that the trigger rearming time is normally below 1 μs, which avoids to miss much PD pulses that arrive narrowly spaced.

The software tool developed by TU Delft reads files and process the data so that the GUI in Fig. 9 is presented to the user. The output of this software tool is a collection of clusters based on the features of the shape of the pulses. Some of the cluster plots that can be computed by the software are the following ones:

(a) *AT plot.* This plot is the time evolution representation of the current peak of each PD pulse.
(b) *QT plot.* This plot is the time evolution representation of the charge of each PD pulse.
(c) *TW plot.* This is the cluster plot of the equivalent time, T_{eq}, and the equivalent frequency bandwidth, W_{eq}, of each pulse as explained in [18–20].
(d) $t_{rise}t_{fall}$ *plot.* This is the cluster plot of the rise time and fall time of each PD pulse.
(e) *IQE plot.* This is the cluster plot of the charge and the energy/charge ratio of each pulse. This is a novel approach for clustering techniques that is suitable for separation of PD sources and that has proven to be resistant to the effect of noise [15].
(f) *FW plot.* This is the cluster plot of the frequency at which the peak of the Fourier spectrum occurs and the equivalent bandwidth.

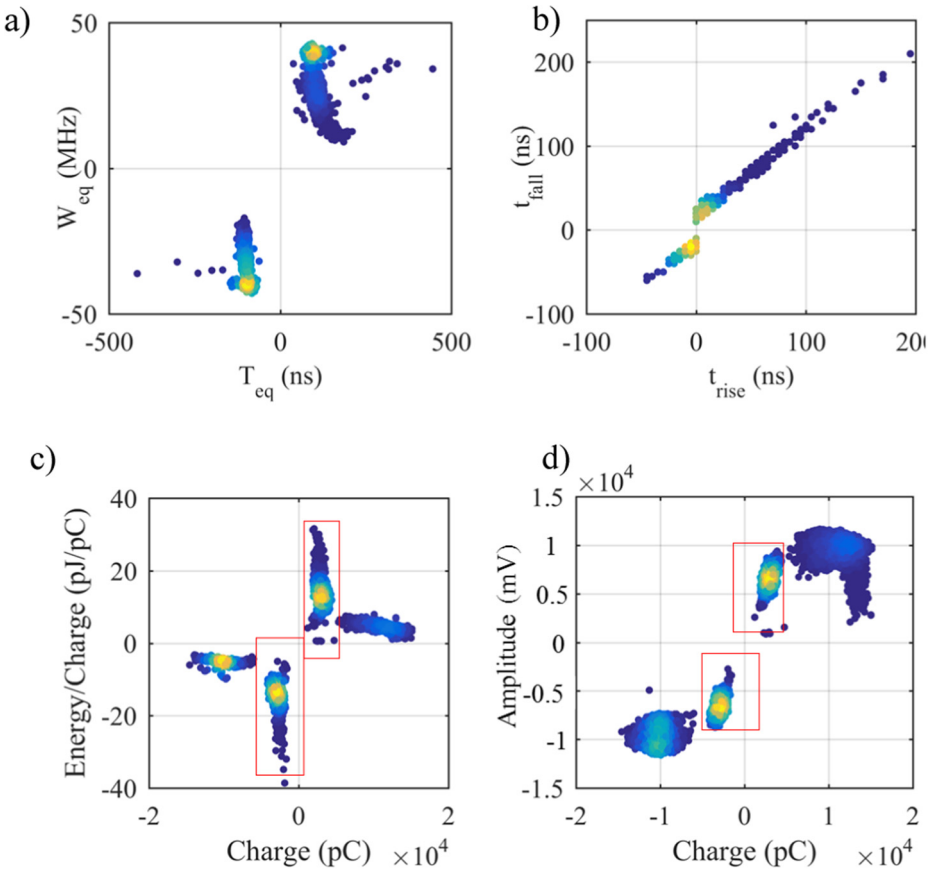

Fig. 14. Cluster plots for the combination of floating electrode and surface discharges, (a) *TW* plot, (b) $t_{rise}t_{fall}$ plot, (c) *EQ* plot, (d) *AQ* plot.

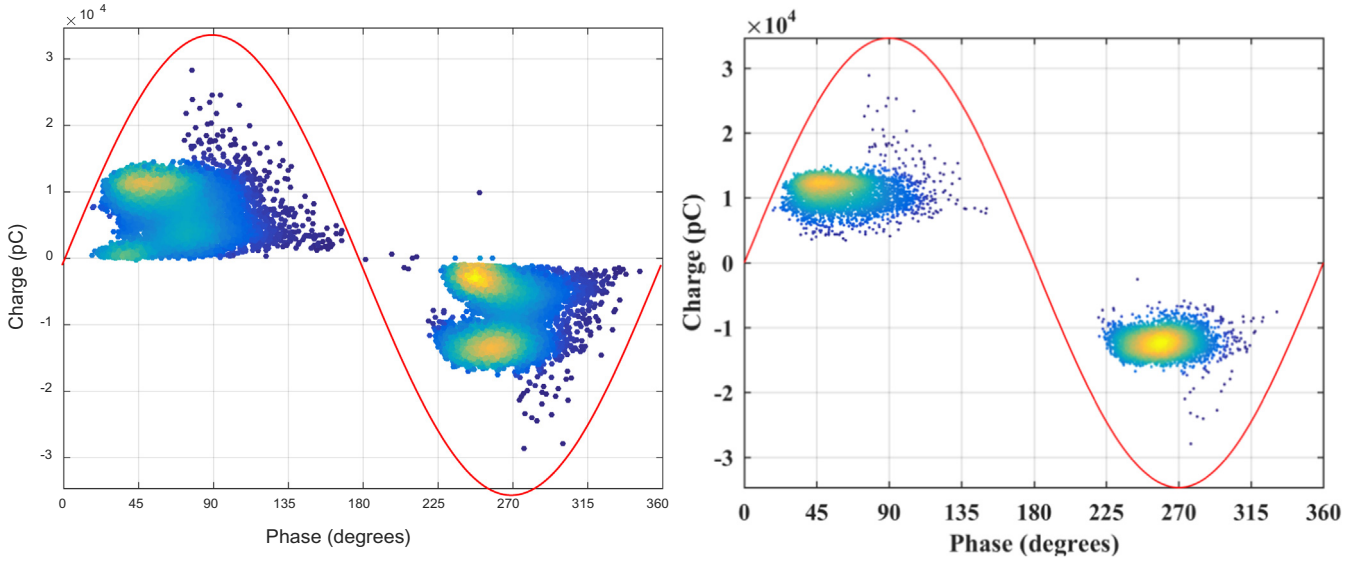

Fig. 15. Left) PRPD pattern for internal discharge and floating electrode combination. (Right) PRPD pattern resulting from the selection within squares in the *TW* plot Fig. 15.

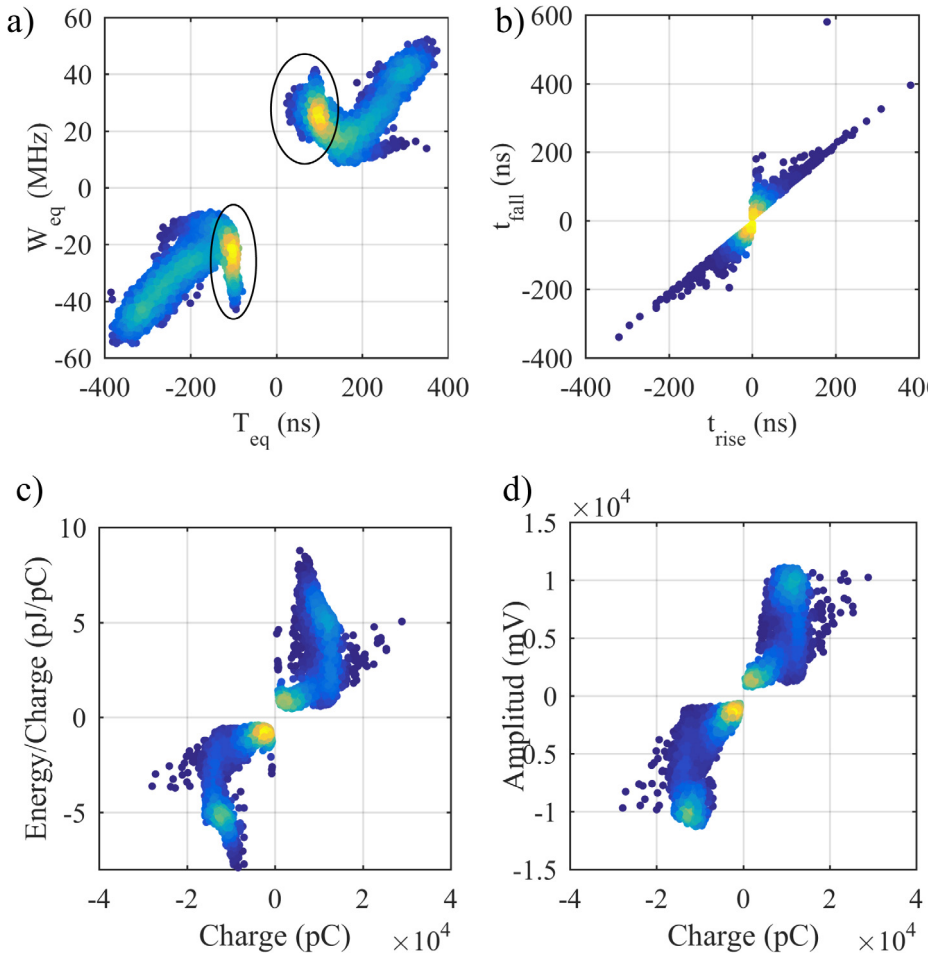

Fig. 16. Cluster plots for the combination of floating electrode and internal discharge, (a) *TW* plot, (b) $t_{rise}t_{fall}$ plot, (c) *EQ* plot, (d) *AQ* plot.

(g) *AQ plot.* This is the cluster plot of the charge and the voltage amplitude of each PD pulse.

4. PD source Characterization by PRPD patterns

From literature is well-known that single PD sources produced characteristic PRPD patterns, which allow easy recognition of them. These patterns as obtained by the test platform are reported in Figs. 10–12. All patterns were made of 50,000 PD pulses and have been recorded at 10 kV. The red sinusoidal waveform is displayed only for phase shift reference. Similar patterns were computed for successive tests due to the fixed location of the PD sources on the test platform that contributes to the measurement repeatability.

5. PD source Characterization by clusters

The test platform provides the option of easily test multiples PD sources which is the most likely case found in HV equipment. When multiple PD sources are active, measurement can result in a rather complex PRPD pattern, not easily matching any of the reference patterns. Therefore, clustering techniques become a necessity and an important tool for PD pattern recognition.

Two cases of multiple PD sources are introduced below as examples of the use of clustering techniques for PD recognition. The first simple example is the combination of surface and floating electrode type PD sources. Fig. 13 shows the PRPD pattern obtained for this combination and Fig. 14 shows the corresponding collection of cluster plots.

Each of the plots in Fig. 14 form clusters that can be better separated and distinguished depending on the PD pulse parameter used. In this case, both PD sources are overlapped in the *TW* plot (Fig. 14a), hindering the separation of each source. The $t_{rise}t_{fall}$ plot (Fig. 14b) offers no chance to separate sources since only one cluster is formed from the rise and fall time features of each pulse.

Plots (c) and (d) in Fig. 14 allow to distinguish the surface discharges from the floating electrode discharges as the features of the pulses form non-overlapping clusters. The software provides the user with a tool to select areas in any of the cluster plots. When the square areas in Fig. 14 are selected, the software retrieves the corresponding PRPD pattern. In this example the pattern is similar to that shown in Fig. 11 (left), so the user can recognize the source as floating electrode discharges.

Other cases as that of Fig. 15 (left) that corresponds to the combination of internal and floating electrode discharges can result in overlapped PRPD patterns. The cluster plots for this combination are shown in Fig. 16. None of the plots enables a straightforward selection of clusters to distinguish each source. However, if the elliptical area in the *TW* plot is selected, the result is the PRPD pattern shown in Fig. 15 (right), which fits well to the pattern for floating electrode discharges as expected.

As can be noted, the aim with the cluster plots is to select those areas that result in PRPD patterns that best fit the reference patterns.

Another tool for the recognition provided by the software tool is the option to compute the clusters individually for both positive and negative discharges. Therefore, in the cluster plots the negative values refer to the parameters computed for negative polarity discharges. In contrast, according to [18], the *TW* plot is computed for the absolute magnitude of all (positive and negative) pulses which would lead to only positive values and possibly to more overlapped clusters. This segregation assists in the separation of the PD sources.

6. Conclusion

The test platform presented in this paper proved to be suitable for research on partial discharge phenomena and for training of students and professionals.

The PRPD patterns shown in Figs. 10–12 validated the design of the constructed electrodes to produce different PD sources. In other words, the patterns obtained for each PD source matched the patterns reported in literature, therefore the test platform performs as expected.

Currently, a wide range of clustering techniques have been developed, tested and used in field tests successfully. However, a factor that hinders comparison or reproducibility of test results is that frequently the effect of measuring circuit is omitted and details of the measuring set-up is not reported. This test platform serves an easy solution to keep constant and minimum the effect of the measuring circuit. The symmetrical and concentric arrangement of the PD sources around the PD coupling capacitor warrants the same circuit parameters for each test and their fixed placement contributes to the repeatability. These features of the test platform are remarkable to assure comparison and reproducibility of test results by other researches. The results also showed that the frequency response of the designed HFCT sensor was suitable to compute the cluster plots shown in Fig. 14 that require to resolve the PD pulses in time for the extraction of PD features.

References

[1] IEC60270. High-voltage test techniques-partial discharge measurements; 2000.

[2] Jürgen F, Neuwersch M, Sumereder C, Muhr M, Schwarz R. State of the art and future trends of unconventional pd-measurement at power transformers. J Energy Power Eng 2014;8(6):1093–8.

[3] Muhr M, Schwarz R. Partial discharge measurement as a diagnostic tool for hv-equipments. In: Int conf prop appl dielectr mater; 2006. p. 195–198.

[4] Meijer S, Agoris PD, Seitz PP, Hermans TJWH. Condition assessment of power cable accessories using advanced VHF/UHF PD detection. In: Conf rec 2006 IEEE int symp electr insul, Toronto, Ont., 2006, p. 482–485.

[5] Muhr M, Strehl T, Gulski E, Feser K, Gockenbach E, Hauschild W, Lemke E. Sensors and sensing used for non-conventional PD detection. In: 2006 Cigre Session; 2006. p. D1–102.

[6] Stone G. Importance of bandwidth in PD measurement in operating motors and generators. IEEE Trans Dielectr Electr Insul 2000;7(1):6–11.

[7] Twiel MM, Stewart BG, Kemp IJ. An investigation into the effects of parasitic circuit inductance on partial discharge detection. In: Proc electr insul conf and electrical manufacturing and coil winding conference, Cincinnati, OH; 2001. p. 213–217.

[8] Rodrigo Mor A, Castro Heredia LC, Muñoz F. Estimation of charge, energy and polarity of noisy partial discharge pulses. IEEE Trans Dielectr Electr Insul 2017;24(4).

[9] Chatterjee B, Dey D, Chakravorti S. A modular approach for teaching partial discharge phenomenon through experiment. IEEE Trans Educ 2011;54 (3):410–5.

[10] Karmakar S. Virtual-instrument-based online monitoring system for hands-on laboratory experiment of partial discharges. IEEE Trans Educ 2017;60 (1):29–37.

[11] Zuberi MU, Masood A, Husain E, Anwar A. Estimation of partial discharge inception voltages due to voids in solid sheet insulation. In: IEEE electr insul conf ottawa, ON; 2013. p. 124–128.

[12] Piccin R, Rodrigo Mor A, Morshuis P, Girodet A, Smith JJ. Partial discharge analysis of gas insulated systems at high voltage AC and DC. IEEE Trans Dielectr Electr Insul 2015;22(1):218–28.

[13] Wang J, Liao R, Wang K, Yuan L, Yang L. Experimental investigations on surface discharge characteristics over oil/pressboard interface based on a rod-to-plane electrode. In: 2014 ICHVE inter conf high voltage eng and appl; 2014. p. 1–4.

[14] Kreuger FH. "Dielectrics", in industrial high voltage. Delft: Delft University Press; 1991. p. 77–96.

[15] Rodrigo Mor A, Castro Heredia LC, Muñoz F. New clustering techniques based on current peak value, charge and energy calculations for separation of partial discharge sources. IEEE Trans Dielectr Electr Insul 2017;24(1):340–8.

[16] Rodrigo Mor A, Morshuis P, Smit JJ. Comparison of charge estimation methods in partial discharge cable measurements. IEEE Trans Dielectr Electr Insul 2015;22(2):657–64.

[17] WG 21. 0. Cigre. Recognition of discharges. Electra, vol. 11; 1969. p. 61–98.

[18] Contin A, Cavallini A, Montanari GC, Pasini G, Puletti F. Digital detection and fuzzy classification of partial discharge signals. IEEE Trans Dielectr Electr Insul 2002;9(3):335–48.

[19] Cavallini A, Contin A, Montanari GC, Puletti F. Advanced PD inference in on-field measurements. I. Noise rejection. IEEE Trans Dielectr Electr Insul 2003;10 (2):216–24.
[20] Rodrigo Mor A, Castro Heredia LC, Muñoz FA. Effect of acquisition parameters on equivalent time and equivalent bandwidth algorithms for partial discharge clustering. Int J Electr Power Energy Syst 2017;88:141–9.

Armando Rodrigo Mor is an Industrial Engineer from Universitat Politècnica de València, in Valencia, Spain, with a Ph.D. degree from this university in electrical engineering. During many years he has been working at the High-Voltage Laboratory and Plasma Arc Laboratory of the Instituto de Tecnología Eléctrica in Valencia, Spain. Since 2013 he is an Assistant Professor in the Electrical Sustainable Energy Department at Delft University of Technology, in Delft, The Netherlands. His research interests include monitoring and diagnostic, sensors for high-voltage applications, high-voltage engineering, and HVDC.

Luis Carlos Castro was born in Cali, Colombia in 1986. He received the Bachelor and PhD degree in electrical engineering from Universidad del Valle, Cali, in 2009 and 2015 respectively. Currently, he is a post-doc in the Electrical Sustainable Energy Department at Delft University of Technology, in Delft, The Netherlands. His research interests include accelerated aging of stator insulation, monitoring and diagnostic tests.

Daniel Antonio Harmsen was born in Willemstad, Curaçao, in 1990. He received the B.S. degree in electrical engineering from the University of the Netherlands Antilles, Willemstad Curaçao, and the Master of Science degree in Electrical Engineering from Delft University of Technology. His main research interests are focused on high-voltage engineering and insulation diagnostics.

Fabio Andrés Muñoz was born in Cali, Colombia, in 1988. He received the B.S. degree in electrical engineering from the Universidad del Valle, Cali, in 2011. He is currently a Ph.D candidate in Electrical Engineering at Universidad del Valle. His main research interests are focused on high-voltage engineering, insulation diagnostics and electrical machines.